LAYERED SILICATE AS A MATRIX FOR GRAPHENE

KULHÁNKOVÁ Lenka[1], TOKARSKÝ Jonáš[2,3], ČAPKOVÁ Pavla[4], MAMULOVÁ KUTLÁKOVÁ Kateřina[2], PEIKERTOVÁ Pavlína[2,3], NEUWIRTHOVÁ Lucie[2], BEŇO Jaroslav[1], STÝSKALA Vítězslav[5]

[1]*VSB - Technical University of Ostrava, Faculty of Metallurgy and Materials Engineering Ostrava, Czech Republic, EU*

[2]*VSB - Technical University of Ostrava, Ostrava, Nanotechnology Centre, Czech Republic, EU*

[3]*VSB - Technical University of Ostrava, IT4 Innovations Centre of Excellence, Ostrava, Czech Republic, EU*

[4]*J. E. Purkyně University in Ústí nad Labem, Faculty of Science, Ústí nad Labem, Czech Republic, EU*

[5]*VSB - Technical University of Ostrava, Faculty of Electrical Engineering and Computer Science, Ostrava, Czech Republic, EU*

Abstract

Montmorillonite was found to be useful matrix for the direct preparation of graphene sheets from conducting polyaniline in the interlayer space of montmorillonite. Oxidative polymerization of the solution of anilinium sulfate by ammonium peroxydisulfate in the presence of montmorillonite particles led to the formation of polyaniline chains both on the surface (revealed by SEM analysis) and in the interlayer space of montmorillonite (proved by a combination of X-ray diffraction analysis and molecular modeling). SEM analysis also showed that superfluous polyaniline created an independent cluster between montmorillonite particles. Such prepared powder material was pressed into tablets using pressure 400 MPa and these tablets were calcined in dynamic argon atmosphere at temperature 1400°C for 1 hour. X-ray diffraction analysis revealed that calcination induced phase transformation of montmorillonite into cristobalite and mullite preserving the layered structure and thus creating good conditions for formation of graphene from polyaniline chains between the silicate layers.

Keywords: montmorillonite, polyaniline, nanocomposite, calcination, graphene

1. INTRODUCTION

Composite materials based on graphene form an interesting group of materials which have great application significance [1]. In literature, attention is given to composites of graphene/polymers [2,3] or graphene/metal oxides [4,5] type. Composites of graphene/non-oxide inorganic matrix type are less common, although they offer a variety of preparation options. One example how to use the structure and composition of the inorganic matrices for the formation of graphene sheets is the thermal decomposition of SiC [6,7]. The main problem in the preparation of graphene-containing nanocomposites is not the actual production of the graphene sheets, but the even distribution of graphene sheets in different matrices. In present work, this problem was solved by intercalation of polyaniline (PANI) into the interlayer space of phyllosilicate. Montmorillonite (MMT), an easy expandable layered silicate, has been chosen as the most convenient silicate matrix for the preparation of PANI/MMT intercalate, i.e. the precursor for the preparation of graphene/silicate nanocomposite. The PANI/MMT intercalate has been subsequently transformed (via high pressure and high temperature treatment) to graphene/aluminosilicate nanocomposite containing graphene sheets adherent to aluminosilicate layers. Hitherto, in the literature has not been published a method for the preparation of graphene/silicate composite based on phyllosilicates. The main advantage of this technology is the low price of input materials.

2. MATERIALS AND METHODS

2.1. Materials and preparation of samples

Na-montmorillonite (MMT) with basal spacing ~ 1.24 nm and structural formula $(Al_{2.85}Mg_{0.71}Ti_{0.02}Fe^{3+}_{0.42})$ $Si_8O_{20}(OH)_4$ with layer charge ~ 0.7 el. per unit cell was purchased from Ankerpoort NV, Netherland. Aniline, ammonium peroxydisulfate and sulfuric acid were used as received from Lach-Ner, Czech Republic. The aniline solution in sulfuric acid and ammonium peroxydisulfate were added into aqueous suspension of montmorillonite (MMT) particles (size fraction < 40 μm) at room temperature. Although the polymerization of aniline was completed within 40 minutes (blue colour of suspension turned into dark emeraldine green – conduction form of PANI), the suspension was stirred for 6 hours. The green solid was collected on a filter by rinsing with distilled water. Resulting powder was dried for 48 hours at 40 °C in a kiln and denoted as PANI/MMT. Pure PANI was prepared in a similar way. The aniline solution in sulfuric acid was mixed with ammonium peroxydisulfate, then the reaction mixture was stirred for 1 hour and the green solid was collected on a filter by rinsing with distilled water. Resulting powder was dried for 48 hours at 40 °C in a kiln and denoted as PANI. Prepared samples were pressed into square tablets using ZWICK 1494 press at room temperature, without any lubrication and binder. Applied pressure was 400 MPa. Controlled pressing (i.e controlled speed of compaction, time, increase and decrease of pressure) was used. Size of each tablet was 28×28 mm and the thickness was 2.708 mm (PANI) and 2.039 mm (PANI/MMT), respectively. Tablets pressed from PANI and PANI/MMT powder were calcined in the furnace of the DIL 402 C/7 dilatometer (Netzsch GmbH, Germany) under the following conditions. The heating and cooling rate was 15 $K \cdot min^{-1}$ with 1 hour long delay at the maximum temperature 1400 °C; protective 99.999% Ar atmosphere with the constant flow rate 20 $ml \cdot min^{-1}$ was used. Non-calcined samples remained denoted as PANI and PANI/MMT and calcined samples were denoted PANI_1400 and PANI/MMT_1400.

2.2. Characterization of structure

Morphology of samples was observed by scanning electron microscope PhilipsXL30 (SEM) equipped with energy dispersive X-ray spectroscope (EDS) and transmission electron microscope Jeol JEM-2010 (TEM). For SEM analysis, samples were coated with an Au/Pd film and the images were obtained using a secondary electron detector. For TEM analysis, samples were dispersed in water. LaB_6 crystal was used as a source of electrons. Accelerating voltages applied to obtain the images from SEM and TEM were 25 kV and 160 kV, respectively. In order to investigate the texture, MMT and PANI/MMT samples were analyzed using combination of X-ray powder diffraction (XRPD) analysis and molecular modeling. X-ray diffraction analysis was carried out in reflection mode using Bruker D8 Advance diffractometer equipped with Co tube ($K\alpha$ = 0.17889 nm) and fast position detector VÁNTEC 1. For the force field calculations using Universal force field [8] as implemented in Materials Studio modeling environment (MS), the model of MMT crystal structure was built according to data published by Tsipursky [9] and Méring [10]. The model was built under the periodic boundary conditions as a 6a × 3b × 1c supercell. Layer charge of the MMT structure arising from the octahedral substitutions was compensated by Na^+ cations and/or PANI chains prepared as dimers of protonated emeraldine salt with charge +4 el. Various space arrangements of the interlayer content (i.e. PANI chains, Na^+ cations, H_2O molecules) were prepared and optimized and basal spacings of the models optimized in MS/*Forcite* module were calculated in MS/*Reflex* module. Calculated and experimentally obtained values were compared in order to find the most probable arrangement of molecules in the interlayer space. Presence of graphene was confirmed using Raman microscope HORIBA XploRATM equipped with 532 nm excitation laser source, with 50× objective and using 1200 mm grating.

2.3. Conductivity measurements

For DC conductivity measurement we constructed special measuring apparatus using DC POWER SUPPLY HY 3003 D-2, Programmable DC POWER SUPPLY BK PRECISION 9120, pA-meter KEITHLEY 6487.

Precision of DC voltage source was 2 ± 10^{-3} V. DC conductivity has been measured in two perpendicular directions, in the tablet plane ($\sigma_{\leftrightarrow}$; Fig. 1a) and in orthogonal direction to tablet plane ($\sigma_{\downarrow}$; Fig. 1a), because due to anticipated orientation of flat MMT particles (as a consequence of pressure; Fig. 1b) higher conductivity in the in-plane direction was expected. Flat Cu electrodes were used for the measurements. The electrodes were polished before each measurement using a special paste.

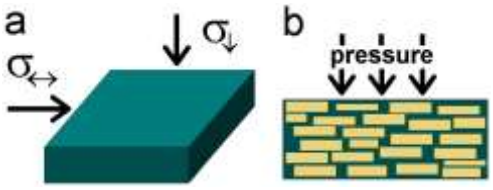

Fig. 1 Schematic illustration: (a) conductivity measurements in two perpendicular directions, (b) ordering of MMT particles in tablet during the pressure.

3. RESULTS AND DISCUSSION

SEM observation revealed the formation of PANI chains on the surface of MMT particles (compare Figs. 2a and 2b) and showed clusters of superfluous PANI between MMT particles (Fig.2b). EDS analysis confirmed presence of PANI in PANI/MMT sample (40.2 wt.% of carbon and 15.44 wt.% of nitrogen). TEM observation of PANI/MMT sample (Fig. 2c) showed that MMT particles are fully covered by PANI but the resolution is not sufficient for direct observation of PANI in the interlayer space of MMT and only weak exfoliation of MMT can be recognized by the naked eye. Nevertheless, changes in basal spacing of MMT were confirmed by XRPD analysis (Fig. 3). Elongated grains of pure PANI can be seen in Fig. 4d and knowing their shape helped us to understand the reason of anisotropy in conductivity observed for tablets pressed from pure PANI (see the discussion of results listed in Table 1).

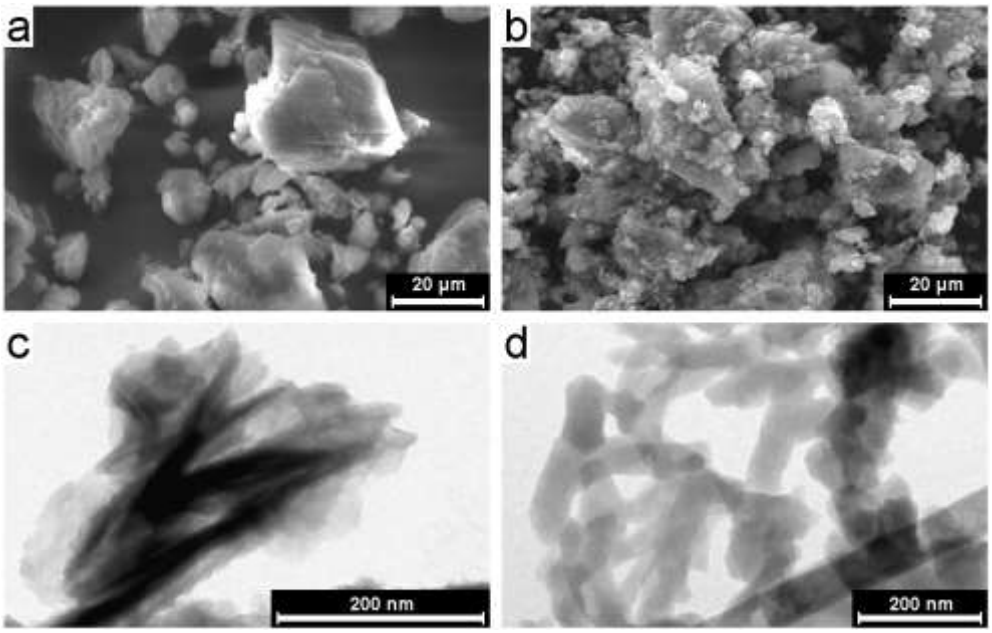

Fig. 2 SEM images of (a) pure MMT and (b) PANI/MMT composite. TEM images of (c) PANI/MMT composite and (d) pure PANI.

Comparison of XRPD patterns of MMT and PANI/MMT samples (Fig. 3) showed that intercalation of PANI and high pressure applied during preparation of tablets resulted in good ordering of MMT particles. The fact that the PANI/MMT structure is homogeneously intercalated was proven by much narrower profile of basal reflection while the the strong texture (caused by high degree of preferred orientation of MMT particles

parallel with the surface of tablet; see Fig. 1b) was proven by the *00l*/*hk*-band intensity ratio. XRPD pattern of pressed PANI/MMT tablet showed the basal spacing d_{001} = 1.285 nm. Calculated value d_{001} = 1.281 nm obtained from the model agreed well with experimental results and revealed parallel arrangement of PANI chains in the MMT interlayer space (Fig. 4). XRPD pattern of PANI/MMT_1400 showed to the destruction of silicate layers and revealed high-temperature phases (mullite, cristoballite) developed during calcination at 1400 °C. Moreover, graphite was also observed in this sample (Fig. 3). Cristobalite phase exhibited strong texture, i.e. cristobalite(101) planes were preferentially oriented perpendicular to the direction of pressure as same as MMT(001) planes before calcination (see Fig. 1b). Type of texture in PANI/MMT_1400 sample was close to PANI/MMT sample because the MMT(001) planes are transformed into cristoballite(101) planes. Top and side views on these two planes (Fig. 3) shows their similarity. Therefore, layers of PANI chains adherent to the silicate sheets were not destroyed and the formation of graphene sheets can occure. Wide and little intense "reflection" located around ~ 15° 2θ suggested the presence of amorphous carbon.

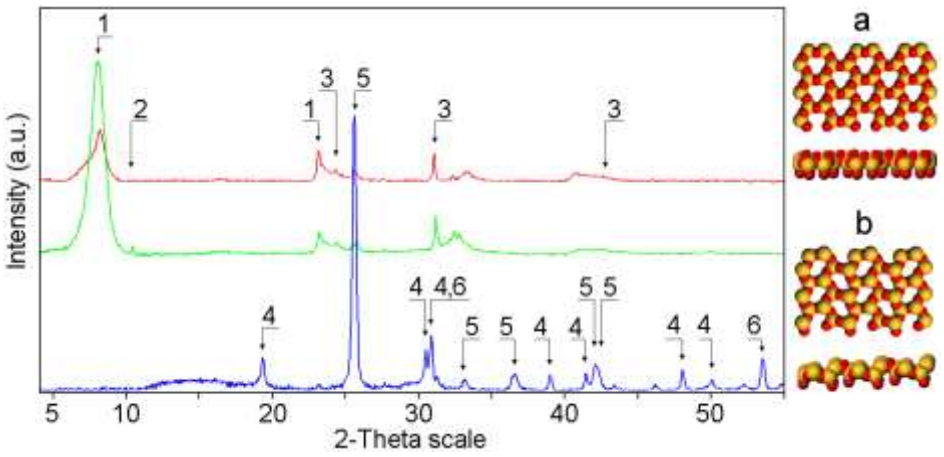

Fig. 3 XRPD patterns of pure MMT (red), dried PANI/MMT (green), and PANI/MMT_1400 (blue). 1 – MMT, 2 – illite, 3 – α-quartz, 4 – mullite, 5 – cristobalite, 6 – graphite 3R-polytype. Top and side views on (a) MMT(001), and (b) cristobalite(101) planes are on the right.

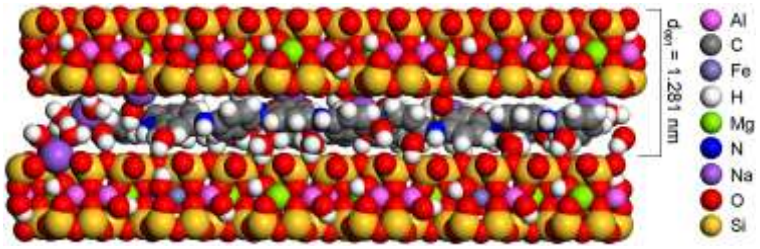

Fig. 4 Optimized model of PANI/MMT structure having d_{001} = 1.281 nm and monolayer arrangement of PANI chains. Water molecules and Na^+ cations attracted by OH groups in octahedral sheets of MMT structure are located close to hexagonal cavities in MMT tetrahedral sheets.

Raman spectra of PANI_1400 and PANI/MMT_1400 samples are shown in Fig. 5. Both spectra showed the disorder band (defects in the samples; ~1350 cm^{-1}) and the graphitic band (orderliness of carbon structure; ~1600 cm^{-1}). More intensive disorder bands revealed the predominance of defects in carbon structure [11,12]. Characteristic bands of PANI chains were not observed in these calcined samples which is understandable. Presence of amorphous carbon (in agreement with XRPD analysis) was revealed by the broadness of bands. The most interesting finding was made in Raman spectrum of the PANI/MMT_1400 - new intensive band with maxima centered at 2701 cm^{-1} (see Fig. 5b). This band is generally ascribed to 2D overtone of graphite but its high intensity is typical for graphene [12-15].

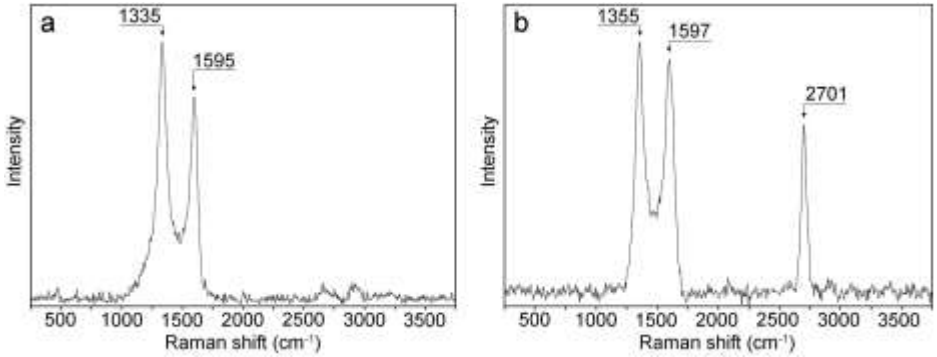

Fig. 5 Raman spectra of (a) PANI_1400, and (b) PANI/MMT_1400 samples.

Conductivities measured in two perpendicular directions (see Fig. 1) and anisotropy factor α (i.e. the ratio $\sigma_{\leftrightarrow}$ / $\sigma_{\downarrow}$) are listed in Table 1. In case of uncalcined samples, PANI exhibited higher conductivity in both directions than PANI/MMT but the α value is higher for PANI/MMT suggesting higher anisotropy of this sample due to the arrengement of MMT particles serving as an insulator in the direction of pressing (Fig. 1). Lower but still distinct anisotropy in case of PANI can be explained by the shape of PANI grains as formed in pure state (Fig. 2d). Similarly to MMT particles, these elongated grains also tend to preferential orientation under external pressure during the preparation of tablets. Table 1 also showed strong influence of calcination on conductivity. While PANI_1400 became isotropic, a dramatic increase in conductivity was observed in case of PANI/MMT_1400. The in-plane conductivity $\sigma_{\leftrightarrow}$ reached 693.41 S · m^{-1} suggesting the formation of graphene sheets between the aluminosilicate layers. Decrease in anisotropy (α is low, but not negligible) can be explained by phase transition of MMT into mullite and cristobalite as proven by XRPD analysis (Fig. 3).

Table 1 Electrical conductivities in two perpendicular directions ($\sigma_{\downarrow}$,$\sigma_{\leftrightarrow}$) and anisotropy factor ($\alpha = \sigma_{\leftrightarrow} / \sigma_{\downarrow}$) for uncalcined and calcined tablets pressed from PANI and PANI/MMT powder samples.

sample	calcination T (°C)	$\sigma_{\downarrow}$ (S·m^{-1})	$\sigma_{\leftrightarrow}$ (S·m^{-1})	α (-)
PANI	uncalcined	0.102	3.50	34
PANI_1400	1400	1.76	1.81	1
PANI/MMT	uncalcined	0.0007	0.03	43
PANI/MMT_1400	1400	78.67	693.41	9

4. CONCLUSIONS

New material with high electrical conductivity has been prepared by the intercalation of layered silicate MMT with PANI, subsequent pressing the powder intercalate into tablets using high pressure 400 MPa and calcination of these tablets at 1400 °C in an inert dynamic atmosphere. Three different types of carbon were found by XRPD analysis and Raman spectroscopy in this material: amorphous carbon, graphite and graphene. We assume that clusters of superflouos PANI chains located between MMT particles were transformed into amorphous carbon while PANI chains forming layers on the MMT surface turned into graphite, and PANI chains in the interlayer space of MMT were transformed into graphene. No graphene was found in calcined tablet prepared from pure PANI. This suggests an important role of the MMT interlayer space where PANI chains can form the monolayers which are during the calcination transformed into graphene sheets. Conductivity measurements showed that while calcined PANI tablet loses the conductivity, PANI/MMT tablet become much more conductive and in the direction parallel to silicate layers the conductivity reached the value 693 S · m^{-1}. This unique method of preparation has one very important advantage which is the low cost of all materials used. However, further research is necessary and

dependence of various calcination conditions, different clays, and PANI / clay ratios on the resulting conductivity will be studied.

ACKNOWLEDGEMENTS

This work was supported by the Ministry of Education, Youth and Sports of Czech Republic project (SP2015/50) and by the European Regional Development Fund in the IT4Innovations Centre of Excellence project (CZ.1.05/1.1.00/02.0070).

REFERENCES

[1] STANKOVICH S., DIKIN D. A., DOMMETT G.H.B., KOHLHAAS K.M., ZIMMEY E.J., STACH E.A., PINER R.D., NGUYEN S.T., RUOFF R.S. Graphene-Based Composite Materials. Nature, Vol. 442, No. 7100, 2006, pp. 282–286.

[2] KIM H., ABDALA A.A., MACOSKO C.W. Graphene/Polymer Nanocomposites. Macromolecules, Vol. 43, No. 16, 2010, pp. 6515–6530.

[3] SENGUPTA R., BHATTACHARYA M., BANDYOPADHYAY S., BHOWMICK A.K. A Review on the Mechanical and Electrical Properties of Graphite and Modified Graphite Reinforced Polymer Composites. Progress in Polymer Science, Vol. 36, No. 5, 2011, pp. 638–670.

[4] WANG D., CHOI D., LI J., YANG Z., NIE Z., KOU R., HU D., WANG C., SARAF L.V., ZHANG J., AKSAY I.A., LIU J. Self-Assembled TiO_2-Graphene Hybrid Nanostructures for Enhanced Li-Ion Insertion. ACS Nano, Vol. 3, No. 4, 2009, pp. 907–914.

[5] JI L., TAN Z., KUYKENDALL T.R., ALONI S., XUN S., LIN E., BATTAGLIA V., ZHANG Y. Fe_3O_4 Nanoparticle Integrated Graphene Sheets for High-Performance Half and Full Lithium Ion Cells. Physical Chemistry Chemical Physics, Vol. 13, 2011, pp. 7170–7177.

[6] EMSTEV K. V., BOSTWICK A., HORN K., JOBST J., KELLOG G.L., LEY L., MCCHESNEY J.L., OHTA T., RESHANOV S.A., RÖHRL J., ROTENBERG E., SCHMID A.K., WALDMANN D., WEBER H.B., SEYLLER T. Towards Wafer-Size Graphene Layers by Atmospheric Pressure Graphitization of Silicon Carbide. Nature Materials, Vol. 8, 2009, pp. 203–207.

[7] GOLER S., COLETTI C., PIAZZA V., PINGUE P., COLANGELO F., PELLEGRINI V., EMTSEV K.V., FORTI S., STARKE U., BELTRAM F., HEUN S. Revealing the Atomic Structure of the Buffer Layer Between SiC (0 0 0 1) and Epitaxial Graphene. Carbon, Vol. 51, 2013, pp. 249–254.

[8] RAPPÉ A.K., CASEWIT C.J., COWELL K.S., GODDARD III W.A., SKIFF W.M. UFF, a Full Periodic Table Force Field for Molecular Mechanics and Molecular Dynamics Simulations. Journal of American Chemical Society, Vol. 114, 1992, pp. 10024–10035.

[9] TSIPURSKI S.I., DRITS V.A. The Distribution of Octahedral Cations in the 2:1 Layers of Dioctahedral Smectites Studied by Oblique-Texture Electron Diffraction. Clay Minerals, Vol. 19, 1984, pp.177–193.

[10] MÉRING J., OBERLIN A. Electron-Optical Study of Smectites. Clays and Clay Minerals, Vol. 27, 1967, pp. 3–25.

[11] CALIZO I., GHOSH S., BAO W., MIAO F., LAU C.N., BALANDIN A.A. Raman Nanometrology of Graphene: Temperature and Substrate Effects. Solid State Communications, Vol. 149, No. 27-28, 2009, pp. 1132-1135.

[12] ZHOU Z., GU H., WANG C., ZHANG J., LV M., HE R. Study on the Synthesis and Surface Enhanced Raman Spectroscopy of Graphene-Based Nanocomposites Decorated with Noble Metal Nanoparticles. Colloids and Surfaces A, Vol. 430, 2013, pp. 103-109.

[13] FERRARI A.C., MEZER J.C., SCARDACI V., CASIRAGHI C., LAYYERI M., MAURI F., PISCANEC S., JIANG D., NOVOSELOV K.S., ROTH S., GEIM A.K. Raman Spectrum of Graphene and Graphene Layers. Physical Review Letters, Vol. 97, No. 18, 2006, pp. 187401-187405.

[14] RAMIREZ C., OSENDI M.I. Characterization of Graphene Nanoplatelets-Si_3N_4 Composites by Raman Spectroscopy. Journal of the European Ceramics Society, Vol. 33, No. 3, 2013, pp. 471-477.

[15] AKHAVAN O. Photocatylytic Reduction of Graphene Oxides Hybridized by ZnO Nanoparticles in Ethanol. Carbon, Vol. 49, No. 1, 2011, pp. 11-18.